

Supplementary Material

Supplementary Data 1: Lung volume measurement optimization

To obtain accurate lung volume, the breathing strategy was optimized with five naive rats. Lung volume calculation was mainly affected by the residual paramagnetic oxygen, which would accelerate hyperpolarized xenon signal decay and reduce the longitudinal relaxation time of hyperpolarized xenon. Hence, the relationship of measured lung volume and xenon flushing times was evaluated. With the flushing times increased, the larger lung volume would be obtained. The measured lung volume will be stable when the flushing times is more than 2, as shown in supplementary Fig. S1. The flushing times of 3 was chosen for lung volume measure. For xenon flushing, the tidal volume is 3 mL, and the other acquisition parameters were the same as described in the section 2.3.

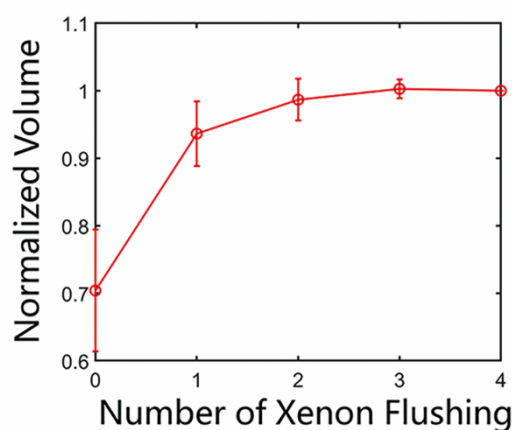


Fig. S1. The relationship of measured lung volume with xenon flushing. Each datapoint was normalized by the max volume, and each data was the average of five rats, shown as mean \pm standard deviation.

Supplementary Data 2: Global and regional lung compliance calculation by CT

The lung parenchyma was obtained by segmenting CT images using Hounsfield Unit (HU) thresholding. Global static lung compliance measured with CT (C_{CT}) was calculated by linearly fitting using the following equation:

$$\Delta V_{CT}(i) = C_{CT} \cdot \Delta P_{CT}(i), i = 1, \dots, n \quad (1)$$

$$\Delta V_{CT}(i) = V_{CT}(i) - V_{CT}(0); \Delta P_{CT}(i) = P_{CT}(i) - P_{CT}(0)$$

Where $V_{CT}(i)$ and $V_{CT}(0)$ are the total lung volume measured using the CT lung images under the airway pressure $P_{CT}(i)$ and $P_{CT}(0)$, $i = 1 \dots n$, respectively; n represents the number of pressure points.

For the calculation of 3D regional lung compliance measured with CT (C_{CT_map}), segmented CT lung images acquired under different airway pressures of $P_{CT}(1)$, ..., $P_{CT}(n)$ were registered to the image with minimal pressure ($P_{CT}(0)$). Then, the Jacobian determinant maps $J(\Psi_{CT-P(i)})$ were calculated from the deformation field $\Psi_{CT-P(i)}$, $i=1 \dots n$, and volume maps were calculated as follows:

$$Vol(P_{CT}(i), x) = J(\Psi_{CT-P(i)}, x) \cdot Vol(P_{CT}(0), x), i = 1, \dots, n \quad (2)$$

where $Vol(P_{CT}(i), x)$ and $J(\Psi_{CT-P(i)}, x)$ are the voxel volume and Jacobian determinant at position x in the CT images under pressure $P_{CT}(i)$, respectively. The C_{CT_map} was calculated by linearly fitting using the following equation:

$$\Delta Vol_{CT}(i, x) = C_{CT_map}(x) \cdot \Delta P_{CT}(i), i = 1, \dots, n \quad (3)$$

$$\Delta Vol_{CT}(i, x) = Vol(P_{CT}(i), x) - Vol(P_{CT}(0), x); \Delta P_{CT}(i) = P_{CT}(i) - P_{CT}(0)$$

where $C_{CT_map}(x)$ represents the lung compliance at position x in the CT image at pressure $P_{CT}(0)$.

Supplementary Data 3: Repeatability of C_{Xe} and C_{Xe_map} measurement

To evaluate the repeatability of C_{Xe} and C_{Xe_map} measurement, ¹²⁹Xe ventilation MRI was repeated in four naive rats for three times. The acquisition parameters and breath strategies were the same with that described in the section 2.3 of the manuscript. The measured C_{Xe} and C_{Xe_map} are summarized in Table S1, and the measured mean coefficient of variation of both parameters was less than 5 %, indicating a good repeatability.

Table S1

Repeated measurement of C_{Xe} and C_{Xe_map}.

	Rat 1	Rat 2	Rat 3	Rat 4
<hr/>				
C _{Xe} (mL/H ₂ O)				
1	0.39	0.46	0.33	0.31
2	0.39	0.45	0.37	0.31
3	0.36	0.45	0.39	0.33
Mean ± SD	0.38 ± 0.02	0.45 ± 0.01	0.36 ± 0.03	0.32 ± 0.01
CV	5.3 %	2.2 %	8.3 %	3.1 %
Mean CV	4.7 %			
C _{Xe_map}				
(10 ⁻⁴ mL/H ₂ O) *				
1	0.47 ± 0.02	0.50 ± 0.02	0.41 ± 0.02	0.34 ± 0.02
2	0.47 ± 0.02	0.51 ± 0.02	0.43 ± 0.01	0.36 ± 0.02
3	0.45 ± 0.02	0.50 ± 0.02	0.46 ± 0.02	0.37 ± 0.02
Mean ± SD	0.46 ± 0.01	0.50 ± 0.00	0.43 ± 0.02	0.36 ± 0.01
<hr/>				

CV	2.2 %	1.0 %	4.7 %	2.8 %
Mean CV	2.7 %			

* C_{Xe_map} is presented as the means \pm SD for the whole lung of each rat.

Fig. S2 shows the C_{Xe_map} and goodness-of-fit (R^2) maps from a representative rat.

The distribution of C_{Xe_map} was similar in three measurements.

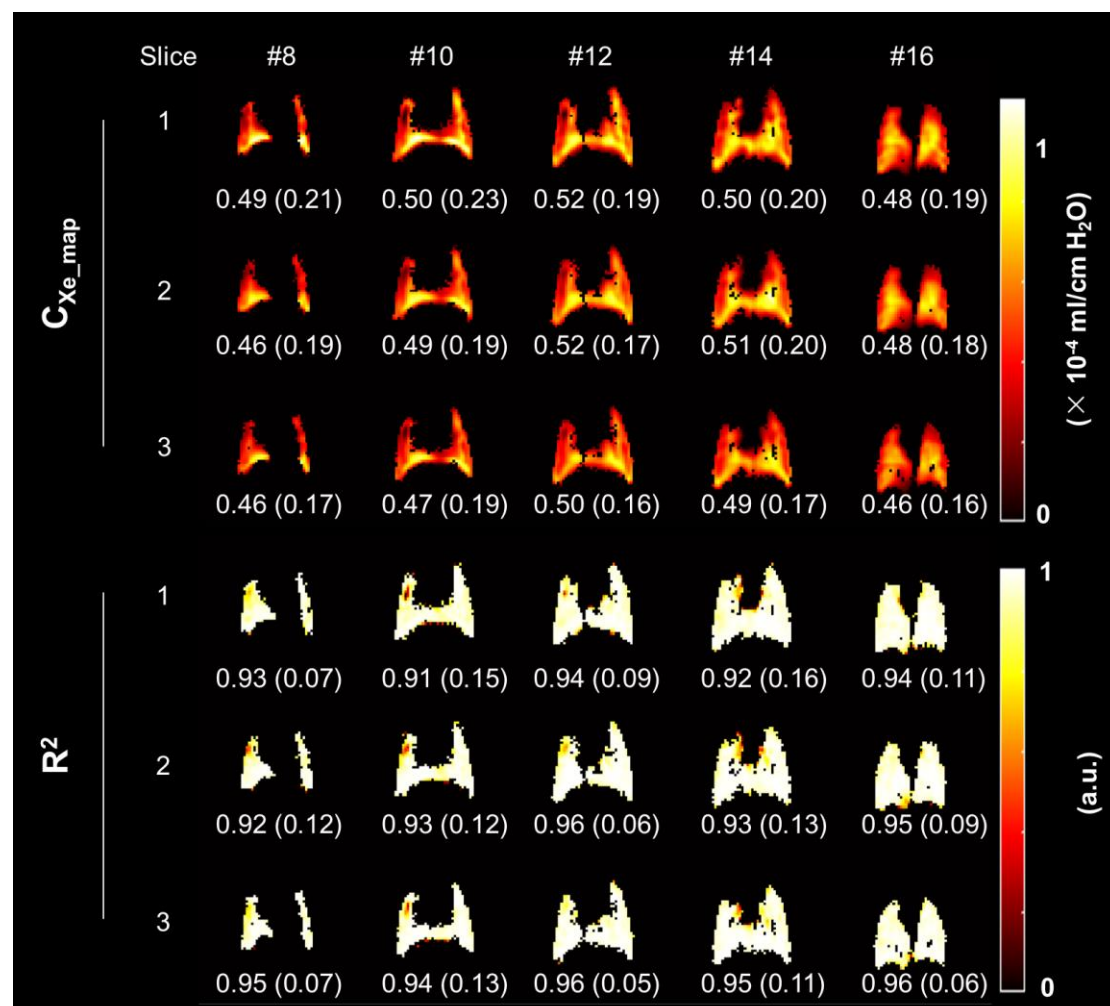


Fig. S2. C_{Xe_map} and goodness-of-fit (R^2) maps from a typical rat. Similar results were found in the three measurements, and the values below each image were the mean \pm standard deviation.

Supplementary Data 4: Test of normality of data in the manuscript

Table S2

Test of normality of data in manuscript.

Method	Parameters	Test of normality Control			Fibrosis		
		S-W test statistic	df	p-value	S-W test statistic	df	p-value
PFTs	IC	0.929	10	0.441	0.934	10	0.486
	FVC	0.987	10	0.991	0.944	10	0.599
	FEV ₁₀₀	0.950	10	0.673	0.978	10	0.954
	TLC	0.916	10	0.327	0.918	10	0.344
	C _{qs}	0.899	10	0.213	0.902	10	0.228
MRI	C _{Xe}	0.943	10	0.588	0.947	10	0.632
	C _{Xe_map}	0.962	10	0.804	0.875	10	0.114
	C_{Xe_map} in apical[#]	0.779	10	0.008	0.963	10	0.822
	C _{Xe_map} in basal	0.964	10	0.834	0.959	10	0.774
	C _{Xe_map} in anterior	0.956	10	0.735	0.967	10	0.857
	C_{Xe_map} in posterior[#]	0.782	10	0.009	0.914	10	0.312
	C _{Xe_map} in right	0.918	10	0.344	0.951	10	0.682
	C _{Xe_map} in left	0.865	10	0.088	0.944	10	0.599
	R _{A-B}	0.909	10	0.273	0.907	10	0.262
	R _{A-P}	0.922	10	0.377	0.888	10	0.161
	R_{R-L}[#]	0.794	10	0.012	0.947	10	0.638
	R² for P-V fitting[#]	0.839	10	0.043	0.899	10	0.211
	Kurtosis	0.940	10	0.555	0.875	10	0.113
	Skewness	0.945	10	0.575	0.942	10	0.576
CT	C _{CT}	0.957	9	0.765	0.873	10	0.191
	C _{CT_map}	0.936	9	0.538	0.895	10	0.107
	C _{CT_map} in apical	0.898	9	0.242	0.951	10	0.682
	C _{CT_map} in basal	0.944	9	0.623	0.917	10	0.329
	C _{CT_map} in anterior	0.971	9	0.903	0.847	10	0.054
	C _{CT_map} in posterior	0.939	9	0.568	0.926	10	0.411
	C _{CT_map} in right	0.955	9	0.741	0.934	10	0.486
	C _{CT_map} in left	0.946	9	0.641	0.888	10	0.161
	R_{A-B}[#]	0.821	9	0.036	0.844	10	0.049
	R_{A-P}[#]	0.901	9	0.257	0.844	10	0.049
	R _{R-L}	0.895	9	0.225	0.912	10	0.294
	R ² for P-V fitting	0.951	9	0.706	0.937	10	0.523
	Kurtosis	0.945	9	0.637	0.962	10	0.808
	Skewness	0.891	9	0.204	0.927	10	0.414
Histology	Septal wall thickness	0.919	10	0.348	0.887	10	0.157

[#] Parameters that are not normally distributed.

Supplementary Data 4: Cross-validation of histological analysis

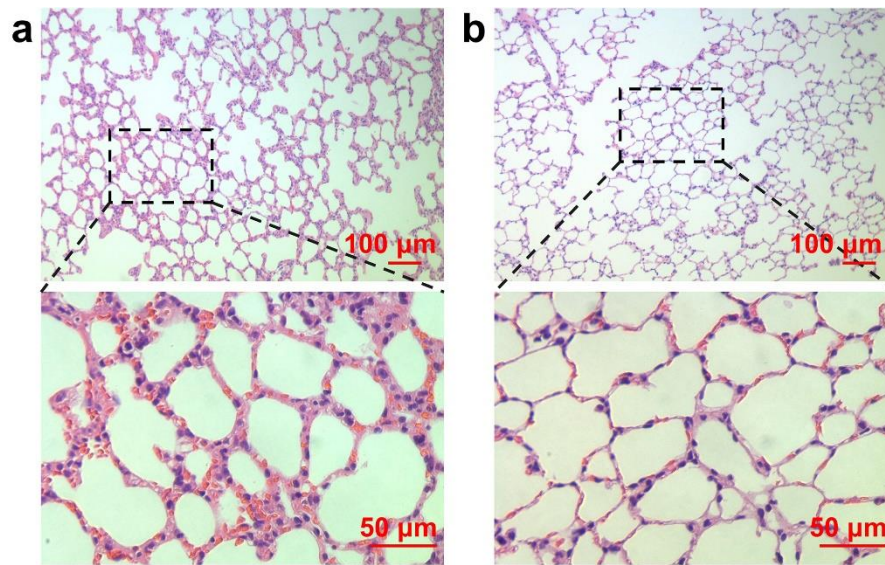


Fig. S3. Typical hematoxylin and eosin (H&E) stained histopathology. (a) fibrosis rat and (b) control rat. The sections from the fibrosis rat showed clear thickening of the alveolar septa compared to the control rat (Top: scale bar = 100 μm , bottom: scale bar = 50 μm).

Supplementary Data 5: Relation between of C_{Xe} and C_{Xe_map} measurement

In C_{Xe} calculation, changes in lung volume are obtained through segmented ventilation images, while changes in lung volume in C_{Xe_map} are derived from Jacobian determinant maps after registration. To validate the consistency between the two parameters, we evaluated the correlation between C_{Xe} and the sum of C_{Xe_map} , as shown in Fig. S4. The results indicate a good consistency between the two parameters ($r = 0.838$).

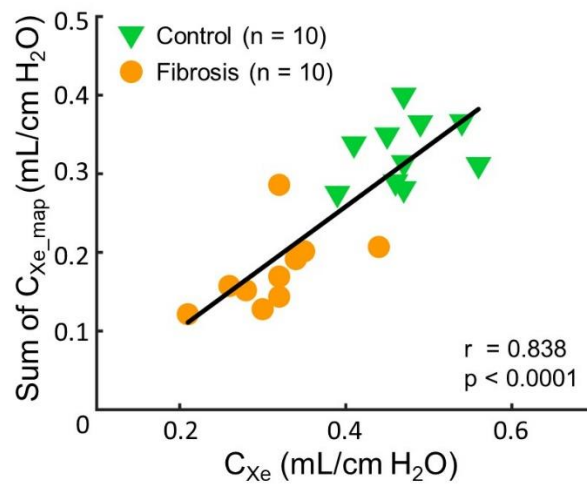


Fig. S4. The correlation between C_{Xe} and the sum of C_{Xe_map} .